Ore Geology Reviews 88 (2017) 43–56

Contents lists available at ScienceDirect

Ore Geology Reviews

journal homepage: www.elsevier.com/locate/oregeo

Low temperature recrystallisation of alluvial gold in paleoplacer deposits

James Stewart [a], Gemma Kerr [a], Dave Prior [a,*], Angela Halfpenny [b,c], Mark Pearce [c], Rob Hough [c], Dave Craw [a]

[a] Department of Geology, University of Otago, Dunedin 9054, New Zealand
[b] Department of Geological Sciences, Central Washington University, 400 East University Way, Ellensburg, WA 98926-7418, USA
[c] CSIRO Mineral Resources, 26 Dick Perry Ave, Kensington, WA 6151, Australia

ARTICLE INFO

Article history:
Received 20 March 2017
Received in revised form 20 April 2017
Accepted 24 April 2017
Available online 25 April 2017

Keywords:
Gold
Placer
Recrystallisation
Dissolution
Precipitation
Deformation

ABSTRACT

Detrital gold particles in paleoplacer deposits develop recrystallised rims, with associated expulsion of Ag, leading to the formation of Ag-poor rims which have been recognised in most placer gold particles around the world. Recrystallisation is facilitated by accumulation of strain energy as the gold particles are deformed, particularly on particle margins, during transportation in a fluvial system. The recrystallisation process ensues after sedimentary deposition and can occur at low temperatures (<40 °C) over long geological time scales (millions of years). In the Otago placer goldfield of southern New Zealand, paleoplacers of varying ages contain gold with varying transport distances and these display differing degrees of rim formation. Narrow (1–10 μm) recrystallised rims with 0–3 wt% Ag formed on gold particles that had been transported <10 km from their source and preserved in Eocene sediments. Relict, coarse grained (~100 μm) gold particle cores have 3–10 wt% Ag, which is representative of the source gold in nearby basement rocks. Gold in the Miocene paleoplacers was recycled from the Eocene deposits and transported >20 km from their source. The gold particles now have wider recrystallised rims (up to 100 μm), so that some particles have essentially no relict cores preserved. Gold in Cretaceous paleoplacers have wide (~100 μm) recrystallised low-Ag rims, even in locally-derived particles, partly as a result of diagenetic effects not seen in the younger placers. Gold particles in all the paleoplacers have delicate gold overgrowths that are readily removed during recycling, but are replaced by groundwater dissolution and reprecipitation on a time scale of <1 Ma. The recrystallisation that leads to Ag-poor rim formation is primarily related to the amount of deformation imposed on particles during sedimentary transport, and is therefore broadly linked to transport distance, but is also partly controlled by the age of the paleoplacer on time scales of tens of millions of years. Gold particles that have been derived directly from basement sources can retain their original composition for long distances (tens to hundreds of kilometres) in a river system, with only minor recrystallised rim development. Gold particles that have been recycled through paleoplacer deposits can lose this link to source composition after relatively short transport distances because of extensive recrystallisation.

1. Introduction

Alluvial gold, and associated concentrations of that gold in placer deposits, occurs as particles distributed among silicate clasts in fluvial gravels. The alluvial gold particles have been derived ultimately from erosion and liberation from hydrothermal gold deposits in basement rocks, with subsequent transportation in downstream river systems for distances ranging from metres to hundreds of kilometres (Knight et al., 1999a; Chapman et al., 2000, 2011; Townley et al., 2003; Garnett and Bassett, 2005; Chapman and Mortensen, 2016). The soft ductile nature of gold ensures that fluvial transportation, with harder silicate clasts, results in substantial shape modification typically forming highly rounded particles and flattened flakes (Knight et al., 1999a; Youngson and Craw, 1999; Chapman et al., 2000, 2011; Townley et al., 2003; Garnett and Bassett, 2005). These distal alluvial gold particles commonly have chemically distinct rims that have apparently formed during or after transport (Desborough, 1970; Giusti and Smith, 1984; Groen et al., 1990; Knight et al., 1999b). The rim compositions are almost pure gold, with lower Ag contents (~1 wt%) compared to typically higher Ag contents (5–50 wt%) in the particle cores, and this phenomenon has been noted in fluvial systems right around the world (Desborough, 1970; Giusti and Smith, 1984; Groen et al., 1990; Youngson and Craw, 1993;

* Corresponding author.
E-mail address: dave.craw@otago.ac.nz (D. Prior).

http://dx.doi.org/10.1016/j.oregeorev.2017.04.020
0169-1368/

Knight et al., 1999b; Chapman et al., 2000, 2011; Chapman and Mortensen, 2016).

Despite the near-universal occurrences of the low-Ag gold particle rims in fluvial placers, the detailed nature and origin of the rims has received little direct study. Desborough (1970) identified the rims with early electron microprobe technology and assumed that the Ag had been leached from the particles. In contrast, some authors have suggested that low-Ag rims have been added to the particles via groundwater-driven Au dissolution and reprecipitation processes that may have involved bacterial mediation (Youngson and Craw, 1993; Falconer and Craw, 2009; Reith et al., 2007, 2012; Fairbrother et al., 2012). Similarly, Groen et al. (1990) invoked self-electrorefining processes, also involving dissolution and reprecipitation of Au, to cause addition of low-Ag rims. These various studies of gold particle rims have generally focused on the chemical differences, although the textures of some delicate micron-scale low-Ag overgrowths attached to the rims clearly indicate that some Au addition has occurred (Falconer and Craw, 2009; Reith et al., 2007, 2012).

In this study, the nature and origin of rims on alluvial gold are investigated by examination of the internal structure of these rims in comparison to the core structure of the particles. A terminological distinction is drawn throughout this study between detrital *particles* and the crystallographic *grains* which make up the interior structure of those particles. The relative crystallographic orientations of the gold grains are a particular focus of the study, along with associated contrasts in gold grain intergrowth textures across the alluvial gold particles. This has been partly achieved using electron backscatter diffraction (EBSD) technology, which enables rapid determination of relative crystallographic orientations of grains *in situ*, with production of micron-scale maps of these relative orientations (Prior et al., 1999; 2009). This technology is combined with associated *in situ* determination of relative compositions of the gold in core and rim of the particles via energy dispersive X-ray spectroscopy (EDS). This combined methodology has been applied to gold particles from the Otago placer goldfield of southern New Zealand, which range in age from Cretaceous to Pleistocene (Fig. 1a-c). The nature of rim formation is noted on gold particles that have undergone differing amounts of fluvial transport and associated physical deformation. Gold from active river systems has been specifically avoided in this study, as those gold particles are regularly reworked with every major storm event. Instead, the focus is on gold particles that have been stored within the older gravels over different amounts of geological time.

2. Geological setting of sampled paleoplacers

The Otago placer goldfield has been derived from orogenic gold deposits in the Mesozoic schist basement, including the world-class Macraes mine (Fig. 1b; Williams, 1974; Craw, 2010). Erosion of those deposits yielded alluvial gold that has formed paleoplacer accumulations in nonmarine sediments that range in age from the Cretaceous to Pleistocene. These placer deposits have been mined sporadically over the past 150 years (Fig. 1b,c; Williams, 1974; Youngson et al., 2006; Craw, 2010). There has been extensive recycling of detrital gold from older sediments to younger sediments as the regional placer goldfield evolved with differential uplift and erosion over 100 million years (Henley and Adams, 1979; Youngson et al., 2006; Craw 2010, 2013). Fluvial sedimentation occurred during extensional tectonism and regional subsidence between the Cretaceous and the Eocene. The goldfield was progressively inundated by marine transgression which was essentially complete in the Oligocene (Fig. 1c; Landis et al., 2008). Renewed uplift under an evolving compressional tectonic regime began in the Miocene and is still active, associated with the modern Alpine Fault plate boundary (Fig. 1a; Jackson et al., 1996; Craw, 2013). Pleistocene-Recent deformation and uplift is occurring as broad (20 km wavelength) folds of basement schist, from which fluvial fans extend into adjacent basins (Fig. 1b; Youngson and Craw, 1993; Jackson et al., 1996; Craw, 2013). The sedimentary cover sequence that hosts the paleoplacer deposits of the Otago goldfield (Fig. 1c) now consists of thin (typically <50 m) remnants of what was never more than a ~300–500 m sedimentary pile (Turnbull, 2000).

Characteristics of the gold particles and host rocks relevant to this study, in the context of the above geological evolution, are summarised in Table 1. Primary hydrothermal gold is typically fine grained (1–10 μm) and encapsulated in sulphide minerals, although minor free primary gold (10–100 μm) occurs in some quartz veins (Craw et al., 2015). However, there has also been extensive supergene alteration of orogenic deposits near to a diachronous unconformity on the schist basement, and this alteration has caused liberation of gold from primary sulphides, and localised enhancement of gold particle size including formation of centimetre scale nuggets (Fig. 2a–c; Craw et al., 2015; Craw and Lilly, 2016; Hesson et al., 2016). Nuggets occur *in situ* in oxidised and clay-altered mineralised zones, and in small streams and colluvium immediately adjacent to the basement sources on actively eroding antiform flanks (Craw et al., 2015; Craw and Lilly, 2016).

Shapes of detrital gold particles derived from both supergene and primary basement sources have been modified with progressive transport distance (Youngson and Craw, 1999). Samples for this study were collected from relatively proximal paleoplacers, wherein the gold has been modified by transport processes to a limited extent, so that some remnants of original basement-sourced gold textures are preserved. The oldest paleoplacer gold is from a locality at Waitahuna (Fig. 1b) which is dominated by locally-derived debris along a normal fault zone (Els et al., 2003). Detrital gold from Eocene quartz pebble conglomerate near Patearoa has a nearby source that is possibly associated with the regional structure that hosts the Macraes mine (Fig. 1b; Craw, 2010). Some of the Eocene quartz pebble conglomerate was eroded and recycled, with its contained gold, into Miocene quartz pebble conglomerate as noted at Garibaldi (Fig. 1b; Craw, 2013). Both the Eocene and Miocene quartz pebble conglomerate deposits have been uplifted by rising antiformal folds during the Pleistocene, with gold and hosting sediments recycled into proximal fluvial fans (Craw, 2013).

3. Methods

3.1. Sample selection

Gold samples were obtained from active and historic mine sites, and from exploration drillholes. Nuggets were found with a commercial metal detector. Samples of finer grained gold were concentrated from hosting debris by water-washing with a traditional gold pan. The collected gold samples were then randomly divided into two groups for either surface examination or interior examination. Gold particles intended for surface examination were mounted onto aluminium stubs using double sided carbon tape and imaged optically with a stereomicroscope before being analysed using the scanning electron microscope (SEM). Gold particles intended for interior examination were sprinkled on to sticky tape so that they did not all lie flat, and even flat flakes were at least partially up-standing. These mounts were then embedded in 25 mm epoxy resin discs that were then ground to expose sections through the particles, and polished with diamond paste. These discs were ground and polished sufficiently deeply to expose sections through the interior of the particles, but it was not possible

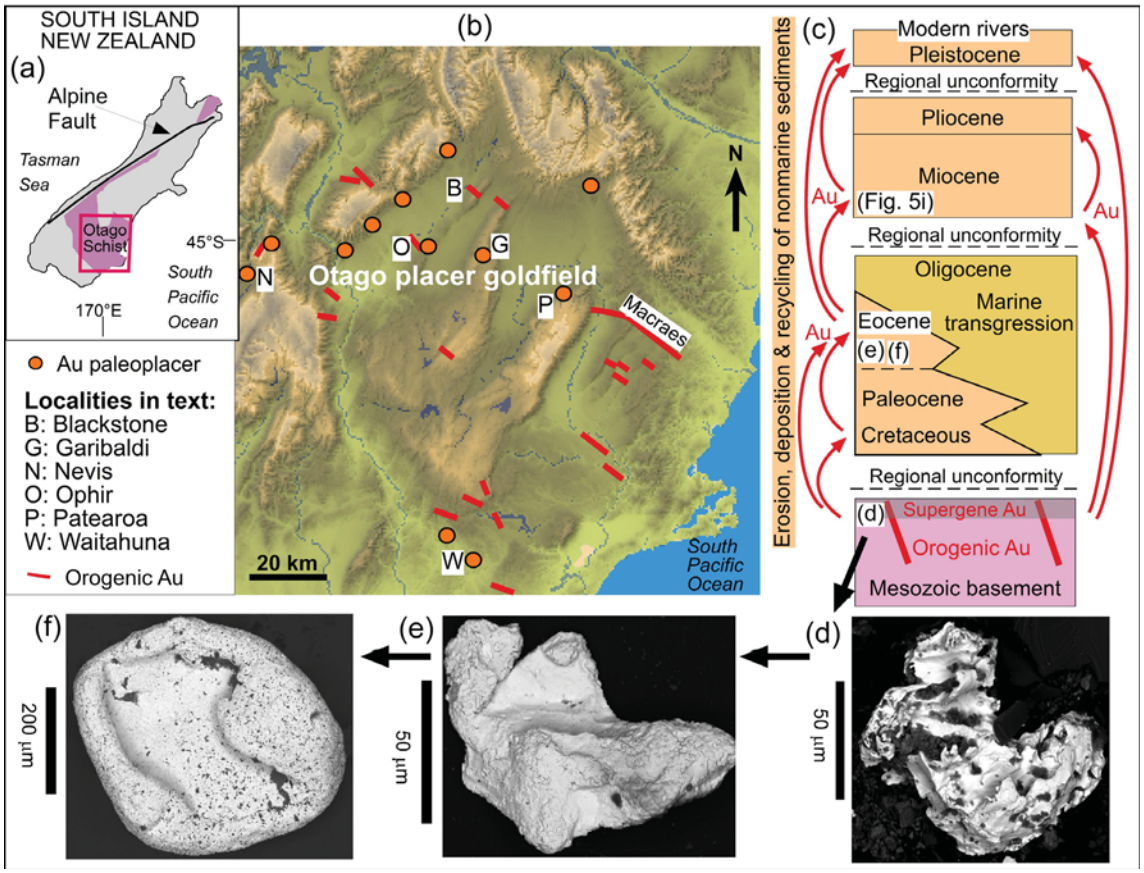

Fig. 1. Location and stratigraphic setting of gold samples examined in this study. (a) Regional setting. (b) Hillshade image of the Otago placer goldfield, with gold localities mentioned in the text and Table 1. (c) Summary stratigraphic column, showing the relationships of host fluvial sediments for paleoplacers of varying ages, with general pathways of detrital gold recycling. (d)–(f) Backscatter electron images of typical gold particles, from basement (d) and variably modified during transport (e, f; as in stratigraphic column in c). Folded flake from Miocene is shown in Fig. 5i.

to ensure that the true centre of the particles were exposed and the resultant sections are necessarily only two-dimensional slices through three-dimensional objects of irregular and unknown shapes. Small gold nuggets were sliced in two with a sharp knife, with one half retained for surface examination and the other half mounted in epoxy resin, ground flat, and polished in the same manner as the finer material.

3.2. Preparation of polished surfaces

The mechanical polishing process causes soft ductile gold to become smeared over the surface of the polished specimen, thereby obscuring the internal structure of the gold. This polishing layer, referred to as the Beilby layer (Beilby, 1903) is at least 1 μm thick, and has to be removed to enable further examination of the original gold grain textures. In this study, we have used two techniques: chemical etching and broad ion-beam polishing (BIBP). We have worked around the advantages and disadvantages of each of these techniques to maximise the information gained from the study.

The simplest, lowest cost, and most rapid technique (minutes) for removing the polishing layer is to etch the specimen in *aqua regia*. This has the advantage of enhancing the grain structure for optical microscopy, and its effectiveness can be monitored during the etching process with a hand lens. The disadvantage of etching is that grain boundaries, and polishing pits and scratches are preferentially etched and enhanced, which can obscure parts of the structure, especially for SEM imaging. We used dilute (50%) *aqua regia* that was aged (>2 years) and therefore of low potency. This enabled slow etching with maximum control of the extent of the etch depth especially when etching several samples at once. For the gold in this study, a light etch (5 min) was insufficient to expose the grain structure for EBSD examination. A heavy etch (15 min) was ideal for enhancing the grain structure for optical examination, but resulted in some loss of resolution for EBSD. A moderate etch (10 min) was a useful compromise for some specimens, but the EBSD results were still not ideal.

BIBP is preceded by chemical-mechanical polishing (CMP) to give a smooth surface (Halfpenny et al., 2013a). BIBP involves abrasion and milling of the surface with argon ions to leave a highly polished surface for crystallographic examination. Disadvantages of this technique are the equipment expense, the long preparation time required (hours), and the subsequent difficulty of determining whether the specimen has been sufficiently abraded to expose the original structure. For the latter issue, it was necessary to subject the specimen to full EBSD analysis in an SEM to see if plausible original grain structure had emerged. Specimens in this study were subjected to CMP and BIBP by the methods of Halfpenny et al. (2013a) in the CSIRO laboratory in Perth, Australia, where the technique was perfected.

3.3. Scanning electron microscopy

SEM examination of the gold samples was conducted at the University of Otago Centre for Electron Microscopy, and the CSIRO, Perth, using similar settings and techniques in both laboratories.

Table 1
Summary of host sediments and characteristic features of gold particles in paleoplacer deposits in this study.

Age of Au & host; locality (Fig. 1b)	Geological setting	Gold particle shape	Gold particle surface texture	Interior gold grain shape, size[#], Ag[*]	Gold rim: Rim width; grain shape, size[#], Ag[*]
Pleistocene/Miocene; recycled quartz pebble conglomerate + schist debris; *Garibaldi*	Proximal fluvial fan; 10–200 m from source	Flakes, refolded flakes	Abraded, scalloped, micron-scale vermiform and crystalline overgrowths	Angular, equant, deformed; 20–100 μm; Ag = 3–10 wt%	Rim 20–100 μm; Grains: angular, equant, undeformed; 1–20 μm; Ag = 0–3 wt%
Miocene; quartz pebble conglomerate; *Garibaldi*	Fluvial paleochannel; recycled Eocene sediments	Flakes, refolded flakes	Abraded, scalloped, micron-scale vermiform and crystalline overgrowths	Angular, equant, deformed; 20–100 μm; Ag = 3–10 wt%	Rim 20–100 μm; Grains: angular, equant, undeformed; 1–20 μm; Ag = 0–3 wt%
Pleistocene/Eocene; recycled quartz pebble conglomerate + schist debris; *Patearoa*	Proximal fluvial fan; 0.5–2 km from source	Subangular, subrounded, rounded, flakes	Abraded, scalloped, micron-scale vermiform and crystalline overgrowths	Angular, equant, deformed; 20–100 μm; Ag = 3–10 wt%	Rim ~20 μm; Grains: angular, equant, undeformed; 1–20 μm; Ag = 0–3 wt%
Eocene; quartz pebble conglomerate; *Patearoa*	Fluvial paleochannel	Subangular, subrounded, rounded, flakes (Fig. 1e,f)	Abraded, scalloped, micron-scale vermiform and crystalline overgrowths	Angular, equant, deformed; 20–100 μm; Ag = 3–10 wt%	Rim ~20 μm; Grains: angular, equant, undeformed; 1–20 μm; Ag = 0–3 wt%
Cretaceous; recycled quartz pebble conglomerate + schist debris; *Waitahuna*	Proximal fluvial paleochannel on fault scarp	Subangular, subrounded, rounded, flakes; diagenetically altered	Abraded, micron-scale overgrowths intergrown with diagenetic matrix	Angular, equant, deformed; 20–100 μm; Ag = 3–10 wt%	Rim 20–100 μm; Grains: angular, equant/elongate, undeformed; < 1–20 μm; Ag = 0–3 wt%
Proximal basement gold liberation from supergene zone; *Ophir*, *Nevis*	Pleistocene colluvium and ephemeral streams	Crystalline nuggets with minor rounded corners (Fig. 2a,b)	Abraded, scalloped, micron-scale vermiform and crystalline overgrowths	Angular, equant, deformed; Ag = 3–10 wt%	None
Supergene, *in situ*; oxidised, clay-altered schist basement & quartz veins; *Blackstone*	Oxidation zone at basement unconformity	Irregular, angular particles (Fig. 1d)	Micron-scale vermiform and crystalline overgrowths	Angular, equant; clay, Fe oxide inclusions; Ag = 3–10 wt%	None
Primary hydrothermal gold in post-metamorphic structures *Macraes*	Mesozoic orogenic systems	Irregular, angular particles; mostly encapsulated in sulphides	None	Angular, equant, deformed; arsenopyrite inclusions; 1–200 μm; Ag = 3–10 wt%	None

[#] Grain sizes from optical and EBSD observations.
[*] Ag contents from EDS spot analyses.

External textures were observed on 3D gold particles mounted on aluminium stubs without carbon coating, and internal textures of gold were examined using the polished epoxy discs after carbon-coating. Both SEM's are fitted with field emission guns and used operating voltage of either 20 or 30 kV. Backscattered electron (BSE) images were obtained of the 3D surfaces and the flat samples produce from both etching and polishing techniques. Energy dispersive X-ray analysis (EDX) analysis of BIBP prepared surfaces was used to map the elemental distributions and reveal the relative Ag contents. These maps were augmented with EDX spot analysis on both SEM instruments. Ag contents can be determined to within ±1 wt%, but for the purposes of this study, we have focused on relative differences between Ag-rich gold (>3 wt%) compared to low-Ag gold (0–3 wt% Ag).

The EBSD datasets of mapping crystallographic orientations were obtained from the same SEM instruments, using a sample tilt of 70°. Instrumentation and methods are described in more detail by Little et al. (2015) for the University of Otago instrument, and Halfpenny et al. (2013b) for the CSIRO instrument. EBSD maps of the grain orientations were obtained by rastering the electron beam across the gold particles in a regular stepped grid. Patterns of diffracted electrons were imaged on a phosphor screen, from which they were recorded digitally, and automatically indexed for gold. The datasets were used to define the network of grain boundaries within the sample. In the maps shown in this study each pixel is coloured according to crystallographic Euler angles (e.g., Mayerhofer, 2005; Prior et al., 2009; Nolze, 2015). In these maps, changes in orientation are shown by changes in colour although the converse is not necessarily true due to the way the colour scheme is constructed. High angle grain boundaries (HAGBs) separate individual grains from each other and in this work that angle is defined as ≥20°. For the purposes of this study, we were concerned only with relative grain orientations, their internal distortions, and the grain sizes as depicted in the Euler maps, rather than absolute crystal axis orientations (cf. Prior et al., 1999, 2009). Many of the black pixels and areas on the EBSD maps reflect the inability of the software to resolve the gold crystallography at that point, and some black areas are inclusions of other minerals, or scratches in the surface.

4. Textures of gold at basement sources

Primary and supergene gold particles are angular and irregular in shape, including some external crystal facets that are especially well developed on the exterior of nuggets of presumed supergene origin (Table 1; Figs. 1d; 2a,b). Primary gold is typically intergrown with, or encapsulated within, sulphide minerals, mainly pyrite and arsenopyrite. Internal structures of supergene particles and nuggets are dominated by coarse grains with irregular straight, stepped, and curved grain boundaries (Fig. 2c). Coarse grains occur right across most particles, and about the edges (Fig. 2c). Primary and supergene gold particles have broadly uniform composition, with Ag contents ranging from 3 to 10 wt% (Table 1). There is little internal variation in Ag contents within individual particles, including on fine grained margins (e.g., bottom of Fig. 2c).

The EBSD maps generally reflect the observations made optically on etched surfaces (Fig. 2d–g). The coarse grain size and general internal crystallographic homogeneity of grains is apparent at a range of scales (Fig. 2d–g). There are broad variations in colours across large grains that reflect slight internal crystallographic distortion on a wavelength of ~100 μm (Fig. 2d–g). Short wavelength

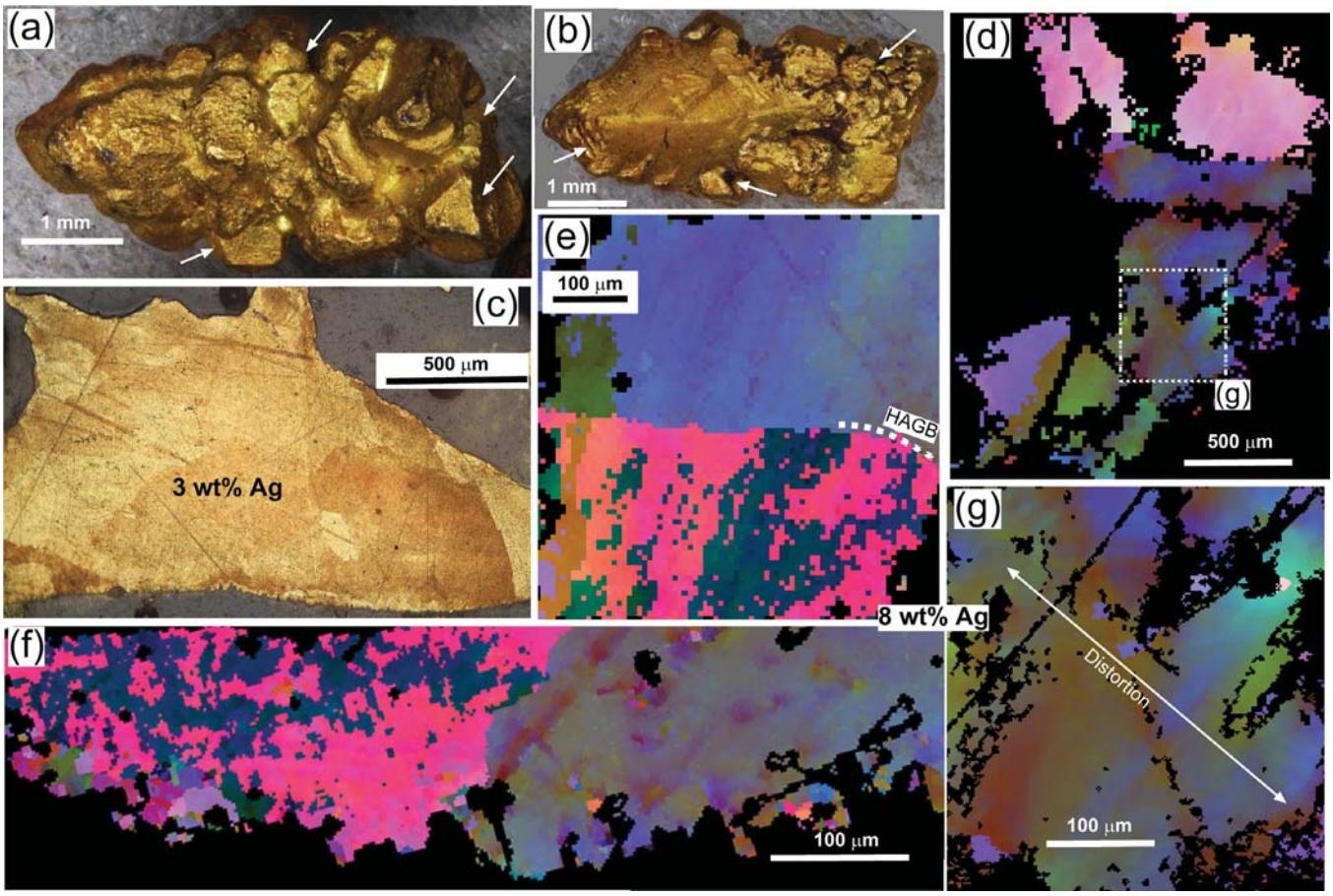

Fig. 2. Gold textures from Otago Schist basement supergene zone (Table 1). (a), (b) Gold nuggets with large crystal shapes, from Nevis locality, with some faceted areas arrowed. (c) Incident light view of a moderately etched section through an *in situ* nugget from Blackstone locality, showing internal structure defined by differential etching of grains with contrasting crystallographic orientations. (d) EBSD crystallographic orientation map of a section through an etched nugget from Ophir locality. (e) EBSD crystallographic orientation map of a prominent high angle grain boundary (HAGB) in nugget in (d). (f) EBSD image of an edge of the nugget in (d). (g) EBSD crystallographic orientation map of large grain in interior of the nugget in (d), with distortion across the grain.

(~1–10 μm) distortions may be artefacts of polishing scratch-related damage.

5. Incipient rim development in proximal detrital gold

The Eocene paleoplacers of the Patearoa area (Fig. 1b; Table 1) consist of quartz pebble conglomerates at the base of a sequence of fluvial to marginal marine sediments (Youngson et al., 2006). These quartz pebble conglomerates rest directly on a schist basement in this area as older sediments were eroded prior to the Eocene. The paleoplacers contain abundant detrital gold particles that are only incipiently rounded and deformed, and many are still subrounded or subangular. Some gold particles contain relict arsenopyrite grains and these have been inherited from some nearby basement source that was presumably primary, rather than supergene. The exact basement source for all these gold particles is not known, but projections of the regional scale structure that hosts the Macraes mine orogenic gold mineralisation zone suggests that a source may be, or may have been, within ~5 km of the Eocene paleoplacers (Craw, 2010). Locally, the Eocene paleoplacers were eroded and recycled into Pleistocene fluvial fans involving transport distances of up to several kilometres (Table 1). The gold particles in the Pleistocene sediments are essentially identical to those in their Eocene source(s).

The internal structure of the Eocene detrital gold particles is dominated by a coarse grained interior with a finer grained rim (Fig. 3a–k). The interior textures include a range of grain sizes, from 20 to 200 μm. Coarse grain boundaries are locally curved, especially near some particle edges, and this curvature is well-defined by some inferred twin planes (e.g., Fig. 3d). Most of the rims fully encircle the particles with a 10–20 μm zone of polyhedral grains that are typically 1–20 μm across. Some rims are only partially formed and the coarse internal grains continue to portions of the edges of these particles (Figs. 3a,j; 4a,b,d). Rims are less obvious on particles with finer grained original interiors, but subtle changes in grain textures generally still distinguish rims around such particles (Fig. 3g). However, some particles are almost entirely fine grained (Fig. 3h,i). Particle rims typically have lower Ag contents (0–3 wt%) than particle interiors (>3 wt% Ag; Table 1) with abrupt changes in composition at the boundaries between rims and interiors.

The differences in grain textures between rim and interior are best displayed with EBSD data (Figs. 3j,k; 4b–e). Interior grains have HAGBs similar to those in basement gold sources (Fig. 2). Large interior grains are commonly internally distorted on >100 μm scale, and this distortion can be highly irregular across grains (Fig. 3j). Fine grained rims have HAGBs and little to no internal distortion (Figs. 3j,k; 4b–e). Small protrusions from the rims consist entirely of fine grained gold (Figs. 3i; 4d). Zones of fine grained gold, similar to those on the rims, can be found superimposed on the coarse grained interiors (Figs. 3c,e; 4c), possibly because the exposed 2D surfaces in the polished specimens are close to the rims.

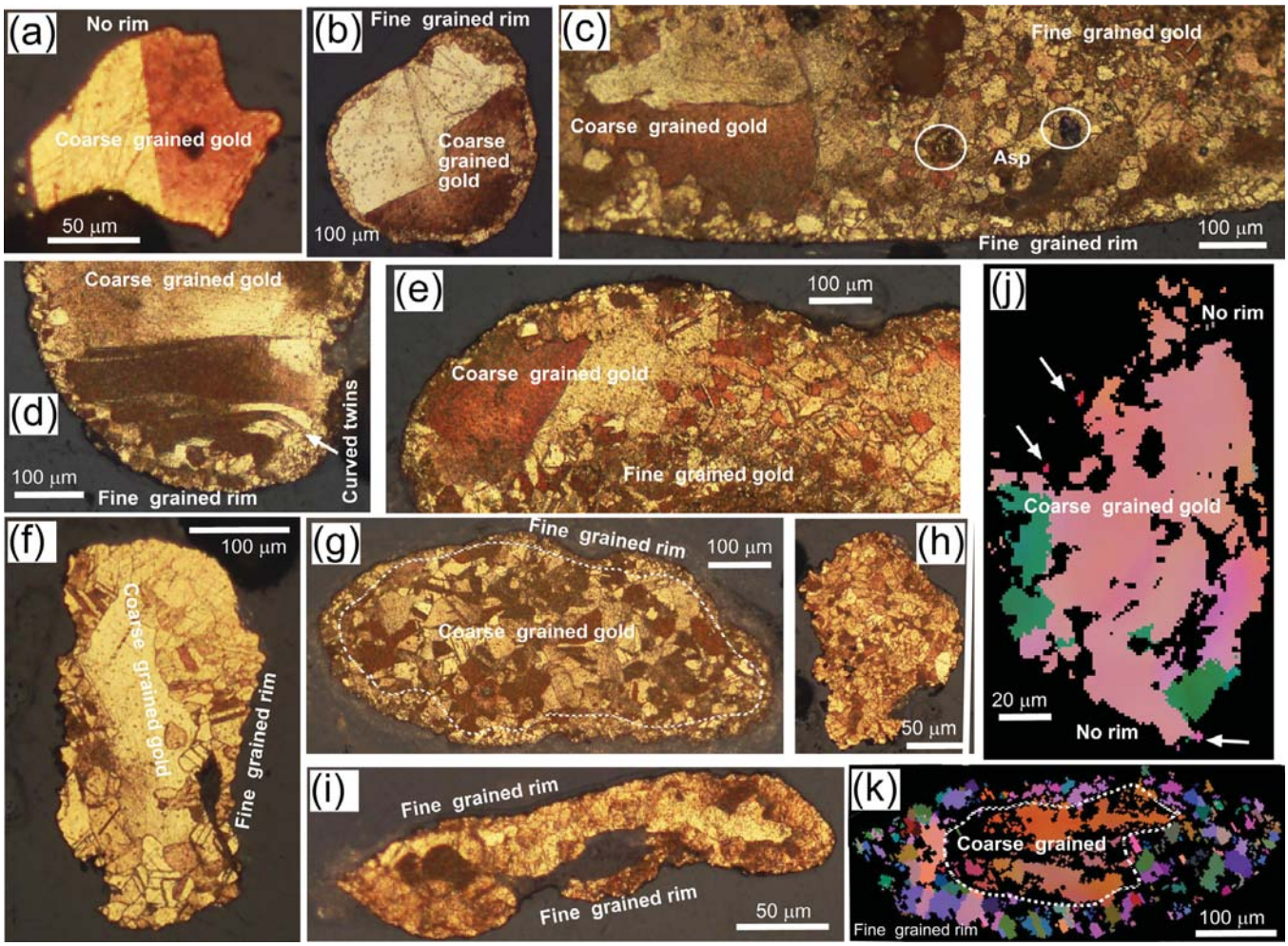

Fig. 3. Interior structure of polished sections through heavily etched proximal detrital gold from Patearoa, showing relict interior coarse grained texture preserved from basement source(s), with variable development of finer grained rims. (a)–(i) Incident light views, showing internal structure defined by differential etching of grains with contrasting crystallographic orientations. Circled dark grains in (c) are relict arsenopyrite (Asp) hosted in finer grained primary gold than that on the left. (j)–(k) EBSD crystallographic orientation maps of grain structure in two different particles. Particle in (j) is essentially a single gold grain that has some distinct crystallographic misalignment. Fine grains with entirely different crystallographic orientations occur on the rims (arrowed). Particle in (k) has a coarse grained core and fine grained rim.

External surfaces of detrital gold particles are typically rounded and abraded, with some scalloped zones on the 1–20 μm scale. Most particle exteriors have numerous cavities and re-entrants, and these are almost invariably filled with sedimentary clay, primarily kaolinite (Fig. 5a–d). Many of these clay-filled cavities contain micron-scale and nanoparticulate gold, either intergrown with the clay or coating the clay surface and the adjacent detrital gold particle (Fig. 5a-d). These gold overgrowths consist of a combination of delicately interlinked irregular vermiform shapes and micron-scale crystals that include subhedral to euhedral hexagonal plates, octahedra, and dodecahedra (Fig. 5a–d). Overgrowths with identical textures occur elsewhere on the detrital gold surfaces, where they locally merge to form continuous exterior coatings, but the clay-related occurrences are the most visually prominent. The overgrowths have low Ag contents, which appear to be near 0 wt% from EDX spot analyses. However, spot analyses of such irregularly-shaped fine grained material are semiquantitative only, as they may be composite analyses that include some of the rim substrate for the overgrowths. Overgrowth textures and compositions are similar on gold particles from Eocene sediments and from nearby Pleistocene sediments (Fig. 5a–d). Similar overgrowths also occur on gold particles derived directly from basement sources into proximal colluvial environments (Table 1; Craw et al., 2016).

6. Enhanced rim development on transported and recycled gold

Detrital gold in the Miocene paleoplacers at Garibaldi historic mine localities (Fig. 1b) has been recycled from Eocene quartz pebble conglomerates similar to those still preserved at Patearoa. The Miocene host sediments are also fluvial quartz pebble conglomerates, and they closely resemble their source sediments: sedimentologically, texturally, and mineralogically. However, there is no overlying marginal marine component to the Miocene sequence, and instead it was overlain by lacustrine mudstones before erosion removed these soft sediments (Youngson et al., 2006; Craw, 2013). The Garibaldi paleoplacers rest directly on schist basement, as all older sediments had been removed by erosion from this portion of the Otago placer goldfield prior to Miocene sedimentation. Pleistocene uplift and erosion has also caused removal of most of the Miocene sequence at Garibaldi, so that only small paleoplacer remnants are preserved in structural depressions. These remnants are largely overlain by thin (<10 m) proximal Pleistocene fluvial fan deposits that contain recycled gold, quartz pebbles, and schist debris, all derived from erosion of nearby Miocene sediments and the underlying basement (Table 1).

Most gold particles from Miocene sediments have been flattened and/or rounded. Many of the resultant flakes have been

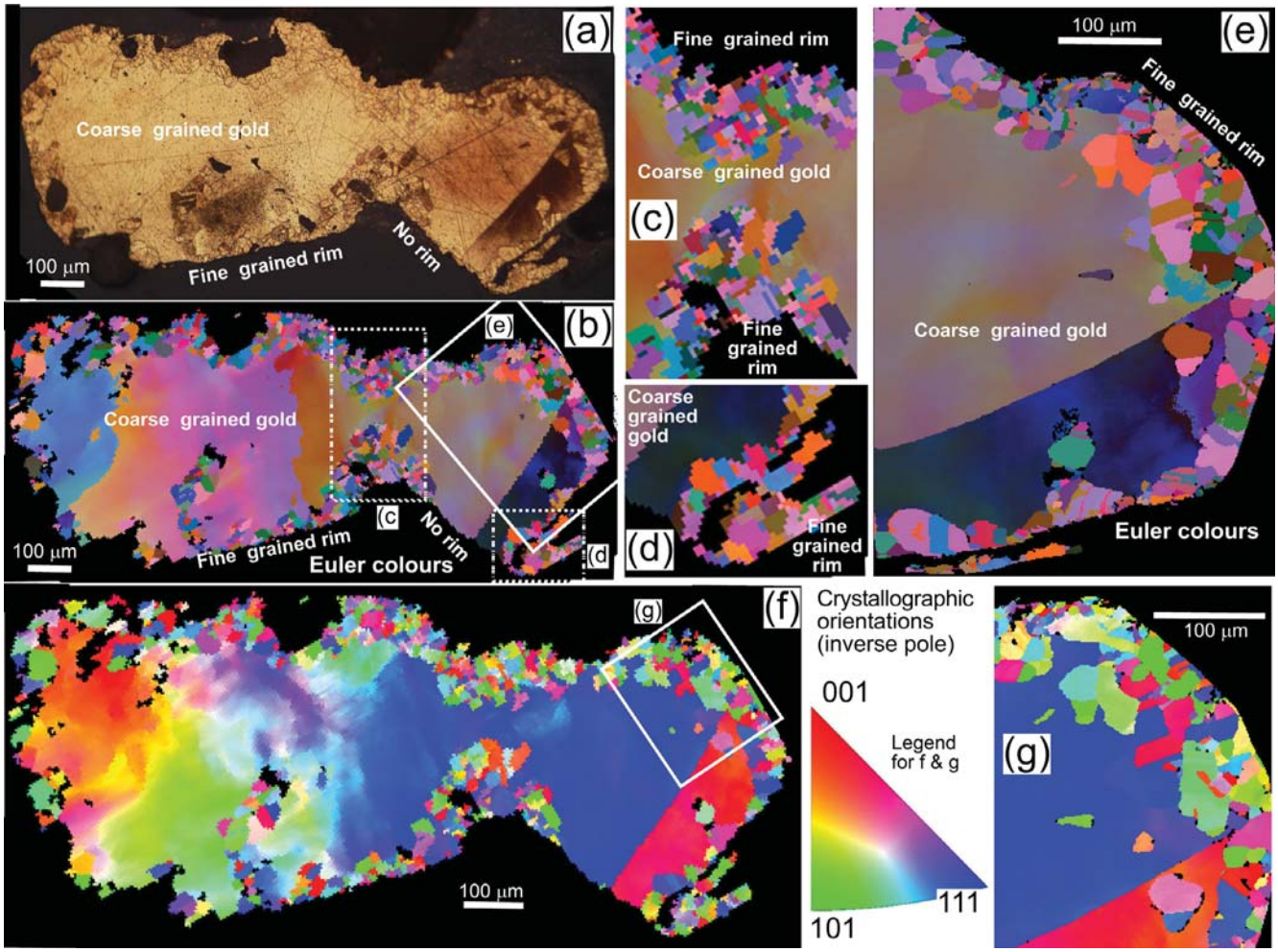

Fig. 4. Interior structure of a polished section through a heavily etched proximal detrital gold particle from Patearoa, (a) Incident light view and (b) EBSD crystallographic orientation map at same scale. More detailed views of portions of the particle are in (c)–(e) to show the contrasts between relict coarse grains and overprinted finer grains. (f), (g) EBSD crystallographic orientation maps coloured for orientations (inverse pole) as in the intervening legend.

folded and refolded to form irregular shapes. Internally, particles have a distinct but irregularly-shaped core zone consisting of silver-bearing gold (typically ~8 wt% Ag), and an Ag-poor rim of varying thickness (Figs. 6 and 7). The boundaries between Ag-bearing and Ag-poor gold are sharp at the micron scale. Zones of low-Ag gold occur in the interior of many particles, and Ag-bearing gold extends to the outer edges in places. Some particles have almost no Ag-bearing gold in their cores, and some particles have no Ag-bearing gold visible, although the sectioned view may not pass through the centre of the particle. Most flattened flakes, or thin protrusions from deformed particles, consist entirely of low-Ag gold (Fig. 7a,d). However, two flakes are notable for having only minor low-Ag gold in patches around their margins (Figs. 6c, 7d).

EBSD maps show that the Ag-bearing gold in the cores is made up of much larger grains than the rims, and that these larger grains are commonly distorted and separated by HAGBs (Figs 6 and 7). The low-Ag particle rims consist of fine-grained gold with widely varying crystallographic orientations, HAGBs, and little to no internal distortion (Figs. 6 and 7). The boundaries between coarse-grained gold and fine-grained gold are sharp, and coincide with the boundaries between Ag-bearing gold and low-Ag rims (Figs. 6 and 7). Hence, for the most part, thin flakes and protrusions are made up of fine-grained gold (Fig. 6a,d), apart from the distinctive elongate Ag-bearing flake that is dominated by coarse grains with HAGBs and only minor internal crystallographic distortion (Fig. 6c).

Gold particles from Pleistocene paleoplacers at Garibaldi have essentially identical internal grain textures and compositions as the gold from nearby Miocene paleoplacers (Figs. 6–8). Likewise the Pleistocene external gold particle textures (scalloped edges, crystalline and vermiform overgrowths) are identical in style, occurrence, and scale to those on gold particles from Eocene paleoplacers (Fig. 5).

7. Particle rims in the oldest paleoplacers

The oldest paleoplacers are Cretaceous in age, and these sediments consist of a combination of locally-derived angular schist basement debris and well-rounded clasts derived from more distant sources (Els et al., 2003). The sediments have undergone substantial post-depositional diagenesis, resulting in a clay-rich matrix and cement (Craw et al., 1995; Kerr et al., 2017). Detrital gold particles are embedded in the clay-rich matrix and exterior gold overgrowths are intimately intergrown with diagenetic clay on the 1–10 μm scale (Kerr et al., 2017). Most detrital gold particles are subangular, exhibit little deformation, have irregular protru-

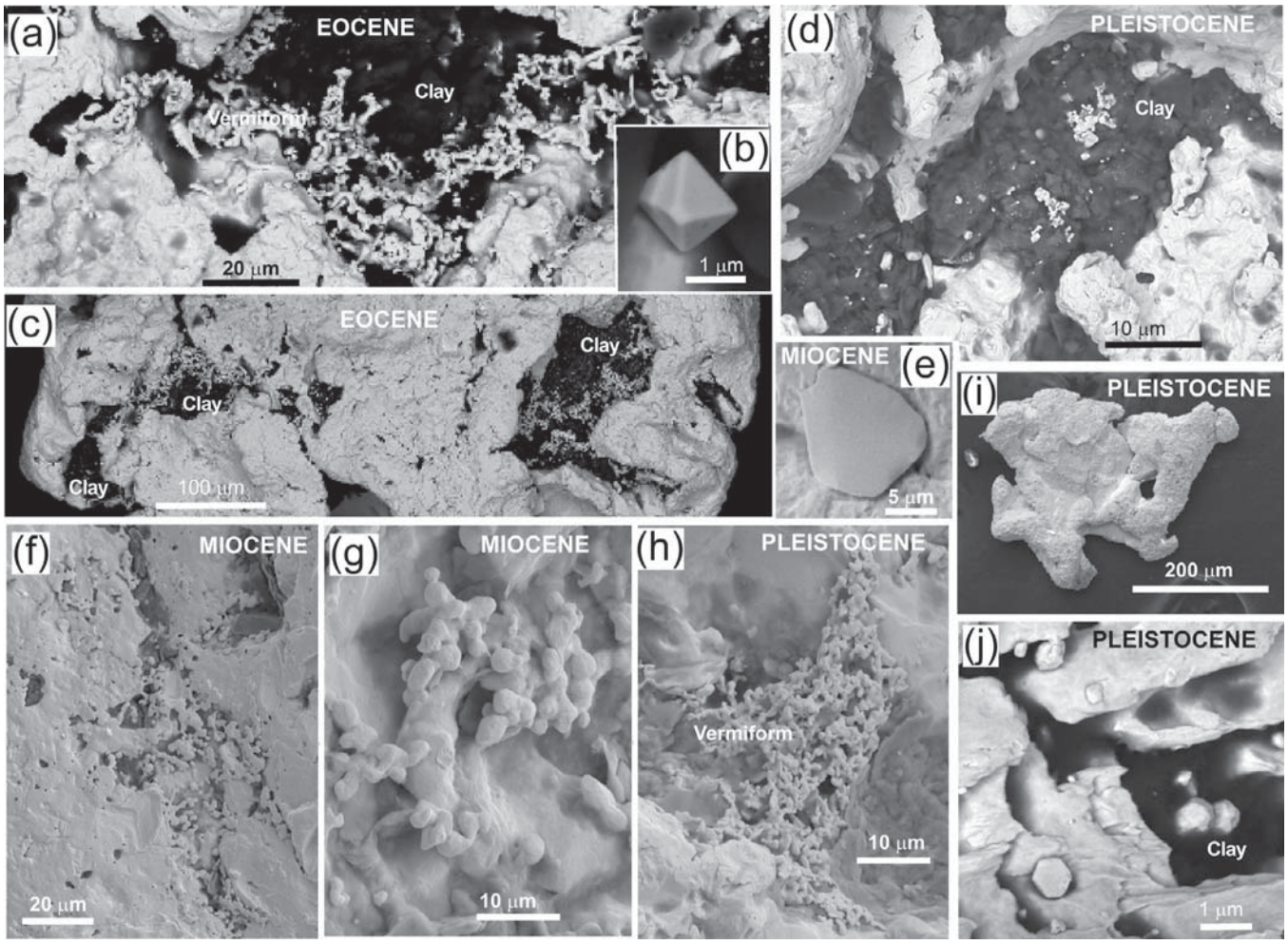

Fig. 5. SEM backscatter electron images of external surfaces of detrital gold (light grey) from Eocene paleoplacers near Patearoa (a–c), a proximal Pleistocene paleoplacer (d) recycled from the Eocene deposits, Miocene paleoplacer at Garibaldi (e–g), and a proximal Pleistocene paleoplacer (h–j) recycled from the Miocene deposit. Subangular gold particles have sedimentary clay (black) in cavities. Vermiform (examples labelled in a & h) and crystalline gold (e.g., in b, e & j) overgrowths are identified, micron scale, at all localities.

sions and inclusions of hydrothermal quartz. Some are well-travelled thin flakes. Hence, the detrital gold has a combination of local and more distant sources, like the hosting sediments.

Internally, many gold particles have a core zone of coarse grained gold, surrounded by a rim of fine grained gold (Fig. 9a–d). In some particles, coarse grained gold locally continues to the particle edge, but most particles are completely coated by the fine grained rims. The boundary between these zones coincides with an abrupt change in Ag content, from Ag-bearing core to low-Ag rims. Thus, the general textural pattern in these gold particles is similar to that in gold from the younger placers although the fine grained rims are generally wider in the Cretaceous paleoplacer particles (up to 100 μm; Fig. 9a). Coarse grains show some crystallographic distortion across grains, whereas finer grains show little to no intragrain distortion and have well-defined HAGBs (Fig. 9b–d).

8. Discussion

8.1. Textural transformations of gold particles

Two distinct sets of processes affected gold particles in the fluvial systems that yielded the paleoplacer deposits in the Otago goldfield: exterior gold overgrowths, and low-Ag rim formation. The exterior gold overgrowths, and associated scalloping of gold surfaces from localised dissolution (Fig. 5) are widespread in the goldfield, and these dissolution-reprecipitation processes have been described previously (Youngson and Craw, 1993; Falconer and Craw, 2009; Craw and Lilly, 2016; Craw et al., 2016). Overgrowths can add a near-complete coating of new gold on the outside of detrital particles, changing their surface textures. However, observations in this study suggest that these processes only resulted in superficial modifications to particle sizes and shapes at the 1–10 μm scale.

Volumetrically more significant are the up to 100 μm wide low-Ag fine grained rims on gold particles (Figs. 3,4,6–8,10a-d). These rims result from substantial internal crystallographic and chemical changes in the gold particles. The fine-grained gold that forms the rims of most particles occurs in zones that commonly mimic the present shapes of grains (Figs. 3,4,6–8). In addition, delicate protrusions from the margins of grains (Figs. 3d,e, 6a) and thin flat flakes (Figs. 7d, 8e) typically consist of low-Ag gold. The fine gold grains in the rims show little or no evidence for internal crystallographic distortion (Figs. 3,4,6–8), so rim formation must have occurred after transport-related gold deformation ceased. Thus, we infer that the rims formed by recrystallisation of deformed gold on the margins of particles, and that recrystallisation occurred *in situ* in the paleoplacers after deposition (Fig. 10c,d). The recrystallisation

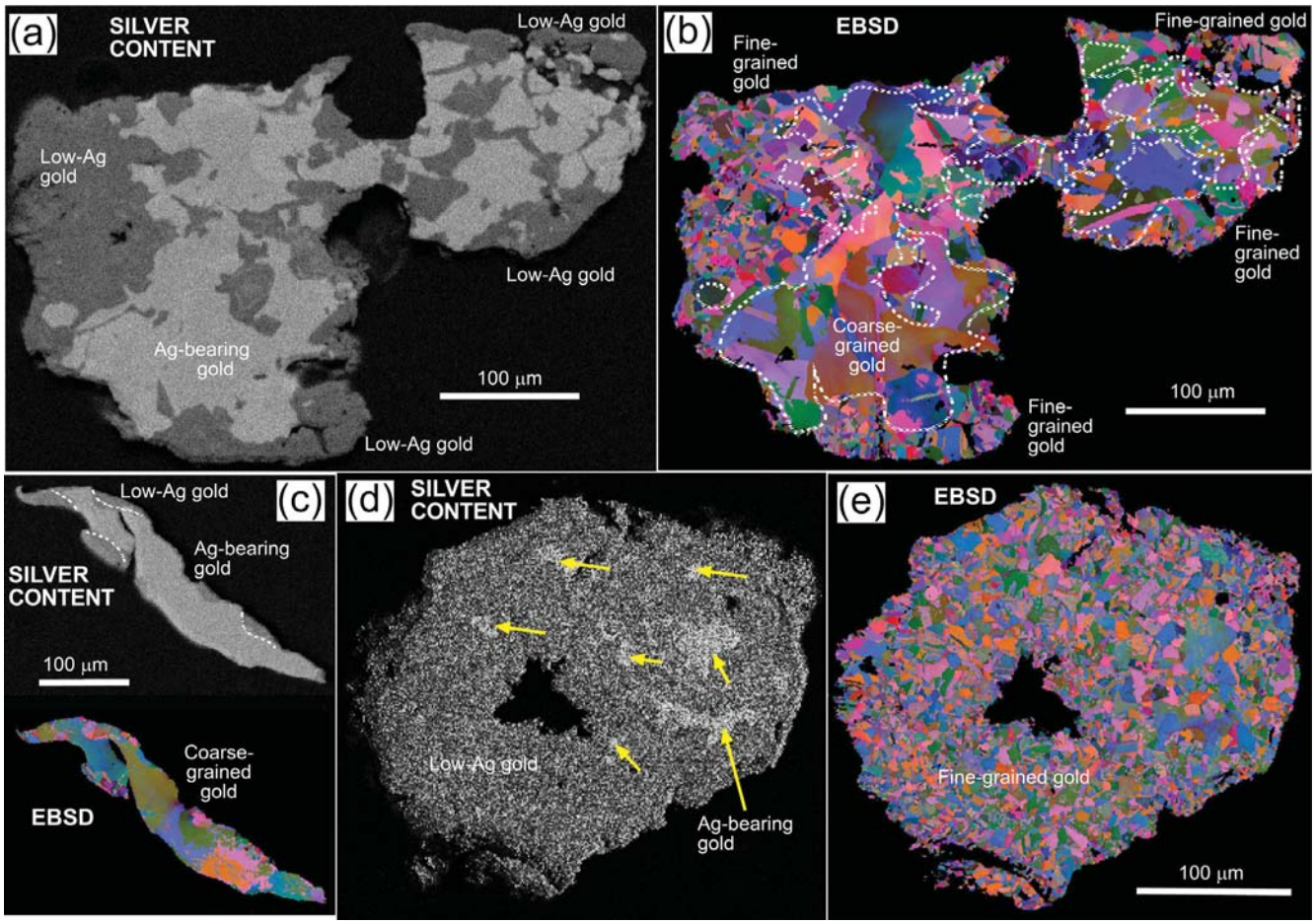

Fig. 6. SEM EDS maps illustrating the relative variations in Ag contents of gold particles from a Miocene Garibaldi paleoplacer deposit, paired with EBSD crystallographic orientation maps of grains. Contrasting Ag contents distinguish Ag-bearing gold (pale) from low-Ag gold (dark). (a, b) Subangular particle with highly irregular boundary between contrasting Ag contents (dotted in EBSD map). (c) Thin gold flake with only minor low-Ag rim development. (d, e) Particle with only small remnant patches of Ag-bearing gold in the exposed part of the interior (arrowed in d).

required nucleation and growth of small new grains and associated grain boundary migration, and this may have been driven by strain energy in the deformed coarse grains (Doherty et al., 1997). Deformation was caused by the repeated impact and abrasion of particles during fluvial transport. The recrystallisation occurred in a sedimentary sequence that was <500 m thick, and parts of it were considerably less than this. Hence, recrystallisation most likely occurred at temperatures <40 °C.

Recrystallisation particle rims has removed almost all evidence of transport-related deformation. However, minor crystallographic distortion and deformation of original grain boundaries persists in the coarse grained interior of the grains (Figs. 3,4,6–8,10b–d). Presumably the strain energy in these portions of the particles was not sufficient to promote more extensive recrystallisation at temperatures <40 °C.

8.2. Chemical transformations

Formation of gold overgrowths on the exterior of particles results from a combination of inorganic chemical reactions and microbiological activity in the groundwater-soaked sedimentary pile (Falconer and Craw, 2009; Reith et al., 2012; Craw et al., 2015; Craw and Lilly, 2016). The groundwater in all the paleoplacer sediments has pH between 6 and 9, and is most commonly near 8, because of the presence of abundant calcite in the basement schists (Craw et al., 2015; Craw and Lilly, 2016). Metastable thiosulphate ions ($S_2O_3^{2-}$) that form during oxidation of primary and authigenic pyrite near to the water table can mobilise Au under the neutral to alkaline pH conditions that prevail in these sediments (Webster, 1986). Similarly, bisulphide ions (HS^-) formed by reduction of groundwater sulphate near to the water table can also mobilise Au in a circumneutral pH sedimentary environment (Webster, 1986; Craw and Lilly, 2016).

The same chemical processes can also mobilise Ag and facilitate its reprecipitation with Au under near-neutral pH conditions (Webster, 1986). Gold reprecipitated by these processes commonly contains some Ag, although generally less than in the host gold (Craw et al., 2015; Craw and Lilly, 2016). The $Ag(S_2O_3)_2^{3-}$ ion is the most soluble complex of the Au-Ag-S-O system, especially under alkaline conditions (Webster, 1986), so some separation of Ag from Au is inevitable at high pH. Partial internal recrystallisation of the gold particles to form the rims involved nucleation of low-Ag gold grains at the expense of the higher Ag contents of the coarser grains (Figs. 6–8). Hence, some Ag was preferentially expelled in solution from the gold particles during this internal recrystallisation process (Fig. 10), reflecting the relatively high solubility of Ag compared to Au in high pH groundwater. The Ag expulsion from within the gold particles during strain-driven solid state recrystallisation may have occurred along the migrating grain boundaries. These processes of recrystallisation and Ag expulsion

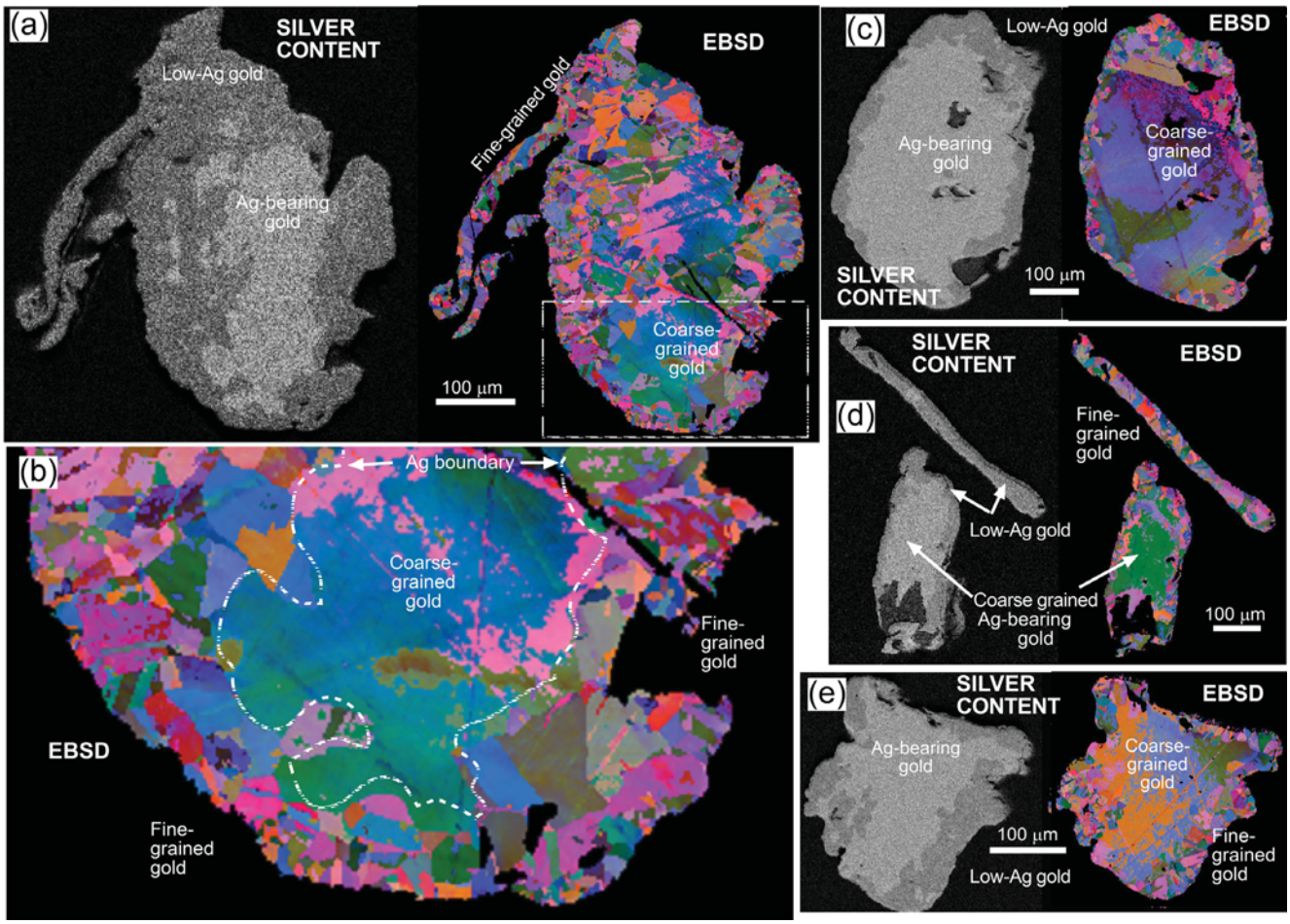

Fig. 7. SEM derived data of interior features of gold particles from a Miocene Garibaldi paleoplacer deposit, with some paired depiction of relative silver contents, and EBSD maps of grains, as in Fig. 6. (a) A small Ag-bearing core is surrounded by low-Ag gold which extends through a delicate and complex protrusion on the margin of the particle. The Ag-bearing gold is coarse-grained, and the low-Ag gold is fine-grained. (b) The EBSD grain size contrast in (a) is shown in enlarged view, with the Ag compositional boundary drawn on in white. Distortion in large grain in the centre causes a gradation of crystallographic orientations across the grain from bottom to top. (c)–(e) Particles with varying widths of fine-grained low-Ag rims, including a flake in (d) with no Ag-bearing core.

were entirely different from those that formed the overgrowths via dissolution of Au and Ag and reprecipitation of the Au onto the exterior surfaces.

8.3. Gold textures and paleoplacer ages

Gold overgrowths formed on detrital gold particles in all the studied paleoplacers regardless of age (Table 1; Fig. 5). Delicate overgrowths are rapidly distorted or fully removed by even small amounts (tens to hundreds of metres) of sedimentary transport (Craw et al., 2016). Since gold particles in the Pleistocene paleoplacers now have delicate overgrowths, those overgrowths must have formed within the Pleistocene sediments after deposition. Hence, overgrowths can form on time scales of tens of thousands to a million years, and are expected on all paleoplacer gold in this environment (Fig. 10c–e). This is in accord with observations of overgrowths formed and reformed on proximal gold nuggets in late Pleistocene sediments (Craw et al., 2016), and rapid overgrowth formation in active rivers (Shuster et al., 2017).

The recrystallised rims on gold in the proximal Eocene paleoplacers examined in this study are narrow, and are distinctly narrower than those in the Miocene paleoplacers (Figs. 3,4,6–8). Some of the particles in the Miocene paleoplacers are almost completely recrystallised (Figs. 6–8), although these observations are based only on two-dimensional sections through portions of three-dimensional particles. However, we infer that the amount of rim recrystallisation is not a direct result of paleoplacer age. Gold particle shapes and observations of geological setting suggest that the Eocene paleoplacers are closer to their source(s) than the Miocene paleoplacers, and the gold in the Miocene sediments has been derived by recycling of the Eocene sediments (Youngson et al., 2006; Craw, 2010). Therefore, the width of the rims on the gold particles probably reflects the greater amounts of physical transport and reworking of the gold in Miocene paleoplacers (Fig. 10d). The greater amount of deformation and particle shape modification of the Miocene gold has imparted more extensive strain-induced recrystallisation and associated expulsion of Ag from the paleoplacers (Figs. 3,4,6–8,10), perhaps culminating in fully recrystallised and Ag-poor particles (e.g., Figs. 7d, 8e).

From the above observations, it is apparent that in the geological context of the Otago placer goldfield, thin (typically ~20 μm) rim recrystallisation occurred after transport of <10 km, and thick (~20–100 μm) rim recrystallisation occurred after recycling and transport of >20 km (Fig. 10a–d). The minor amount of transport and reworking of gold from Eocene and Miocene paleoplacers into proximal Pleistocene sediments (kilometre scale transport) has had no additional effects on rim development. However, some subangular gold particles in Cretaceous paleoplacers, implying limited

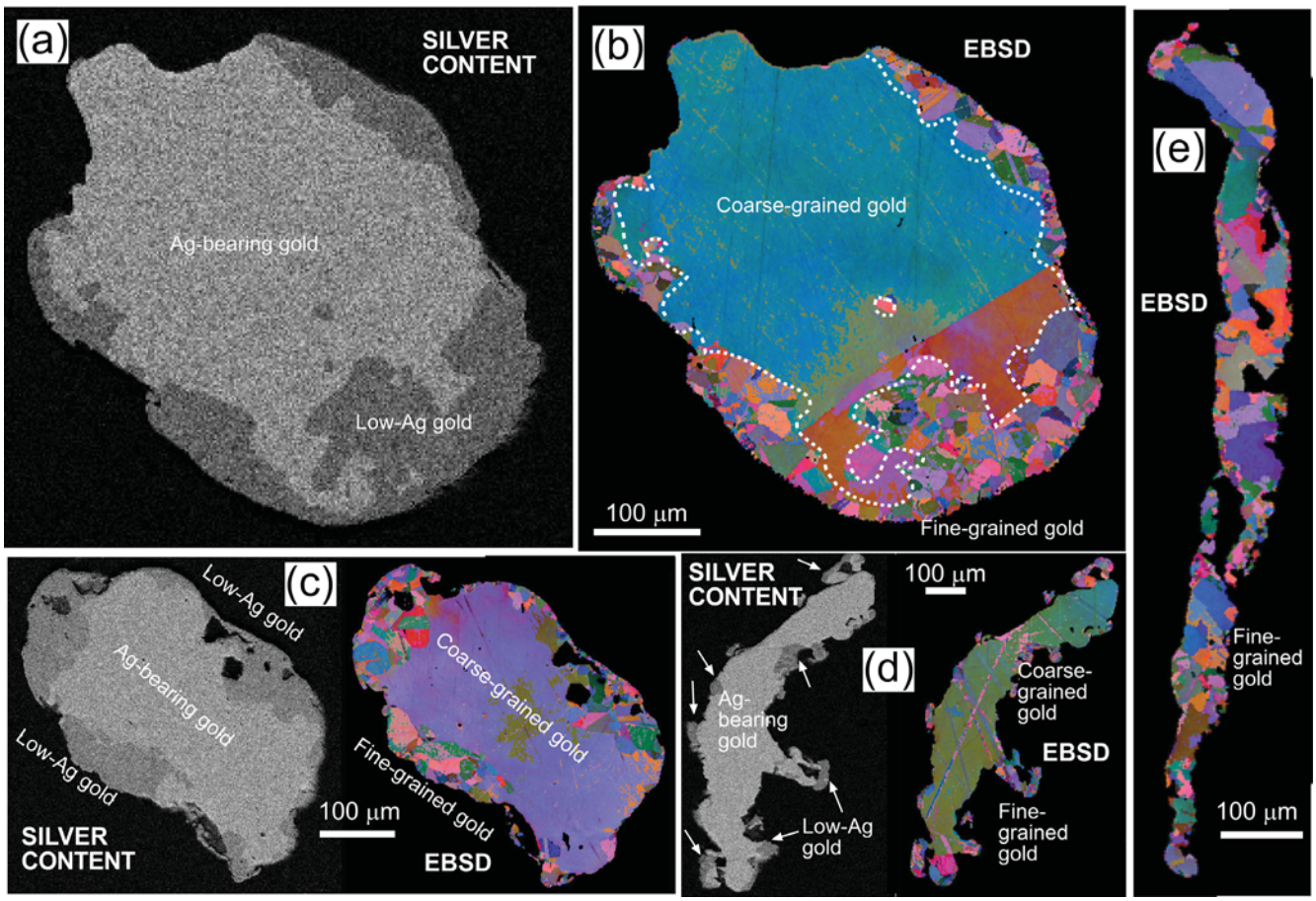

Fig. 8. SEM images of interior features of gold particles from a Pleistocene Garibaldi paleoplacer deposit, with (a)–(d) showing paired depiction of relative silver contents and EBSD crystallographic maps of grains, as in Fig. 6. (e) Thin flake is predominantly fine grained low-Ag gold.

transport from basement sources, have wide recrystallised rims (>100 μm; Fig. 9a). Further, the boundaries between recrystallised rims and relict cores are more gradual in the Cretaceous paleoplacer gold (e.g., Fig. 9b; Kerr et al., 2017) than in the younger examples in this study (Figs. 6–8). These observations suggest that gold recrystallisation does continue with time, especially associated with low-temperature diagenesis as in the Cretaceous paleoplacers (Table 1). The widths of recrystallised rims apparently reflect both physical transport distance and time since deposition, although the effect of the latter may only be observable in placer deposits older than 50 million years.

8.4. Linking placer gold to basement sources

Occurrences of placer gold can be a useful indicator of the existence of undiscovered gold deposits in basement rocks, and this approach has been used in a wide variety of geological settings around the world (Boyle, 1979; Knight et al., 1999a,b; Chapman et al., 2000; Townley et al., 2003; Garnett and Bassett, 2005; McClenaghan and Cabri, 2011; Chapman and Mortensen, 2016). Use of gold compositions is especially useful for placers with relatively short transport distances from sources with distinctive geochemical and mineralogical signatures (1–10 km scale; Knight et al., 1999a; Chapman et al., 2011; Chapman and Mortensen, 2016). In this study, we show that gold transported up to 20 km, with at least one stage of recycling, followed by burial and partial recrystallisation over 20 million years, still retains some record of the grain size and composition of the original basement source (Figs. 6–8). However, in the context of the Otago placer goldfield, this is approaching the maximum useful transport distance for prospecting purposes, as some gold particles have been largely recrystallised throughout (Figs. 6d, 7d, 8e). Moreover, it is essential to identify the original composition within the particles by sectioning them and not just relying on chemical analyses on grain exteriors which are almost certainly compromised by recrystallization and overgrowths in even the most recent of deposits (Shuster et al., 2017).

Long distance transport of placer gold involves substantial shape changes and repeated flattening, folding, and refolding (Boyle, 1979; Knight et al., 1999b; Youngson and Craw, 1999; Townley et al., 2003; Garnett and Bassett, 2005). Indeed, it is the repeated flattening process and resultant increase in flake surface area that aids the on-going entrainment and transport of gold particles in rivers with downstream decrease in gradient (Youngson and Craw, 1999). In this situation, complete recrystallisation of particles should be expected to occur eventually. This recrystallisation may not happen in the transporting river, and our observations suggest that burial and preservation of placer gold for at least millions of years, and possibly tens of millions of years, is required for extensive low-temperature recrystallisation of deformed gold particles. On the other hand, almost all detrital gold particles, even in active river systems, have undergone some rim formation (Desborough, 1970; Giusti and Smith, 1984; Groen et al., 1990; Youngson and Craw, 1993; Knight et al., 1999b; Chapman et al., 2000, 2011; Chapman and Mortensen, 2016) and the width of this rim may increase with increasing transport dis-

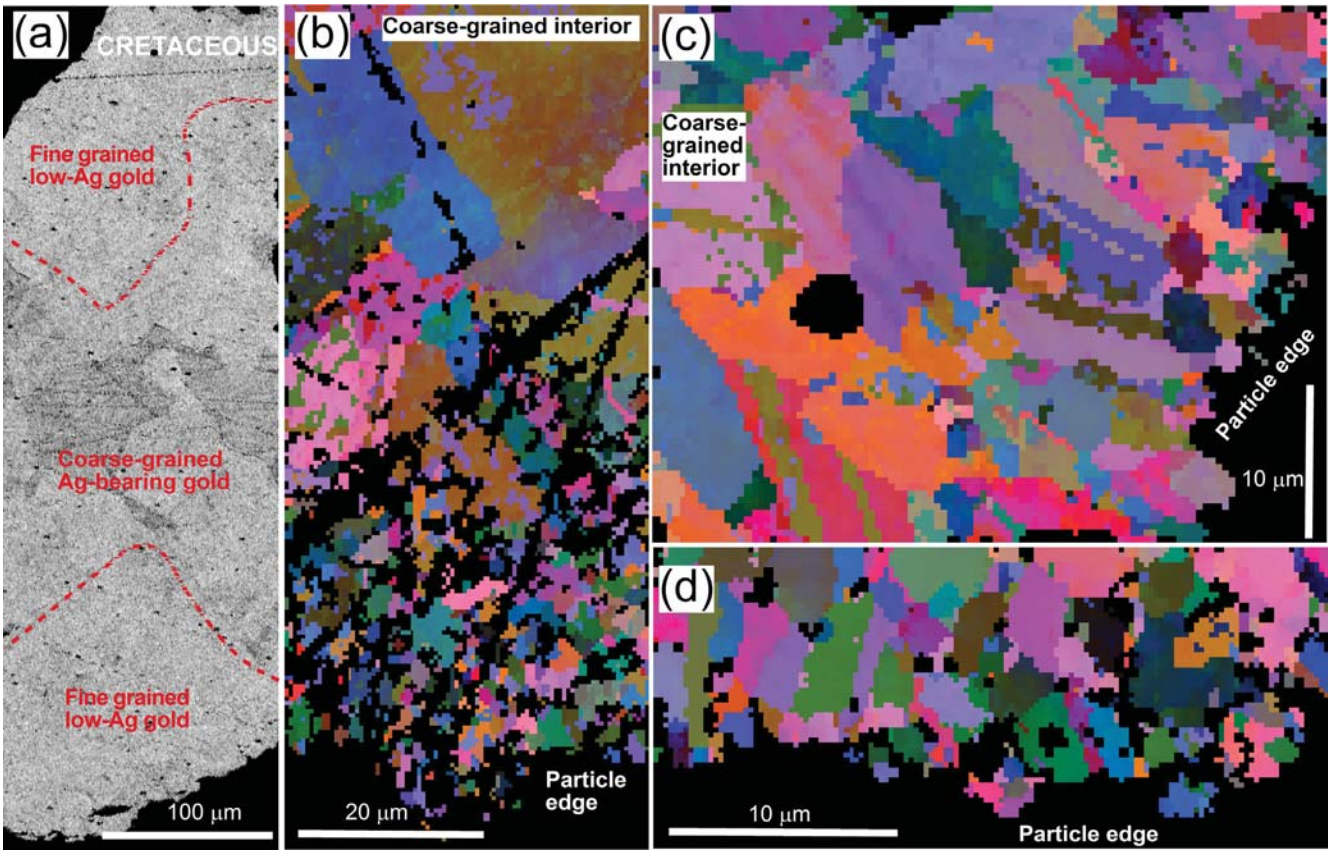

Fig. 9. SEM images of the interior structure of gold particles in a moderately etched polished section from a Cretaceous paleoplacer at Waitahuna locality. (a) Backscatter electron image of a profile across a particle, showing the coarse-grained Ag-bearing core, fine-grained low-Ag outer zones, and the sharp boundary between these (red dashed lines). (b)–(d) EBSD crystallographic orientation maps of portions of particles, showing the grain size and texture contrasts between coarse grained interiors and fine grained outer zones. (For interpretation of the references to colour in this figure legend, the reader is referred to the web version of this article.)

tance and repeated refolding. Nevertheless, gold particles derived directly from basement sources and transported in modern rivers can be expected to retain some evidence of their source deposit composition despite this rim recrystallisation and Ag loss. If the gold has been recycled from intermediate paleoplacers, however, there may have been complete recrystallisation and the link to original source gold composition will have been lost.

These processes and inferences apply for fluvial transport of gold. Long distance transport of gold by glaciers, especially the continental scale ice sheets of the Northern Hemisphere Pleistocene, will have had little or no effect on gold particle compositions via the processes described above. However, once the gold was released into glacial outwash fluvial systems, substantial deformation of particles will have occurred, making that gold prone to recrystallisation and progressive rim development.

9. Conclusions

Gold in orogenic and associated supergene basement sources in the Otago goldfield of southern New Zealand has a coarse grain size (~100 μm) and Ag content between 3 and 10 wt% (e.g., Fig. 10a). Erosion and transport of gold particles for short distances (<10 km) into Eocene paleoplacer deposits caused internal deformation of grains, especially near the edges of the particles (e.g., Fig. 10b). Rims of fine grained (~1–20 μm) recrystallised gold formed around the edges of the particles at some time after deposition of the gold in the Eocene sediments (e.g., Fig. 10c). Recrystallisation was driven by stored strain energy in the more highly deformed marginal grains. The more weakly deformed Interior grains show some crystallographic distortion but have not recrystallised (e.g., Fig. 10b,c). Rim recrystallisation was accompanied by expulsion of Ag in solution, and the rims now have 0–3 wt% Ag.

The gold in a nearby (20 km distant) Miocene paleoplacer has undergone more extensive recrystallisation (e.g., rims are up to ~100 μm wide; Fig. 10d) than the gold in the proximal Eocene deposits. Some gold in the Miocene deposits has almost fully recrystallised to fine grained low-Ag gold, with few or no remnants of the original basement source characteristics are preserved (e.g., Fig. 10e). Gold particles in Cretaceous paleoplacers also have wide low-Ag rims (~100 μm) despite some of that gold having been sourced locally with short transport distances, because of subsequent diagenetic alteration. Gold in all the Otago paleoplacers has some delicate gold overgrowths on exterior surfaces as a result of a combination of dissolution and reprecipitation of gold by groundwater (Fig. 10c–e). Overgrowths can form and reform on a time scale of <1 Ma.

The Otago paleoplacer observations show that major recrystallisation of deformed detrital gold particles can occur at low temperatures (<40 °C) but may require long time, possibly thousands to millions of years. The amount of recrystallisation that occurs is partly affected by transport distance, which imparts the strain energy to the marginal grains (Fig. 10a–e). Extensive recrystallisation may also occur during low temperature diagenesis of paleoplacers over very long time scales (>50 Ma).

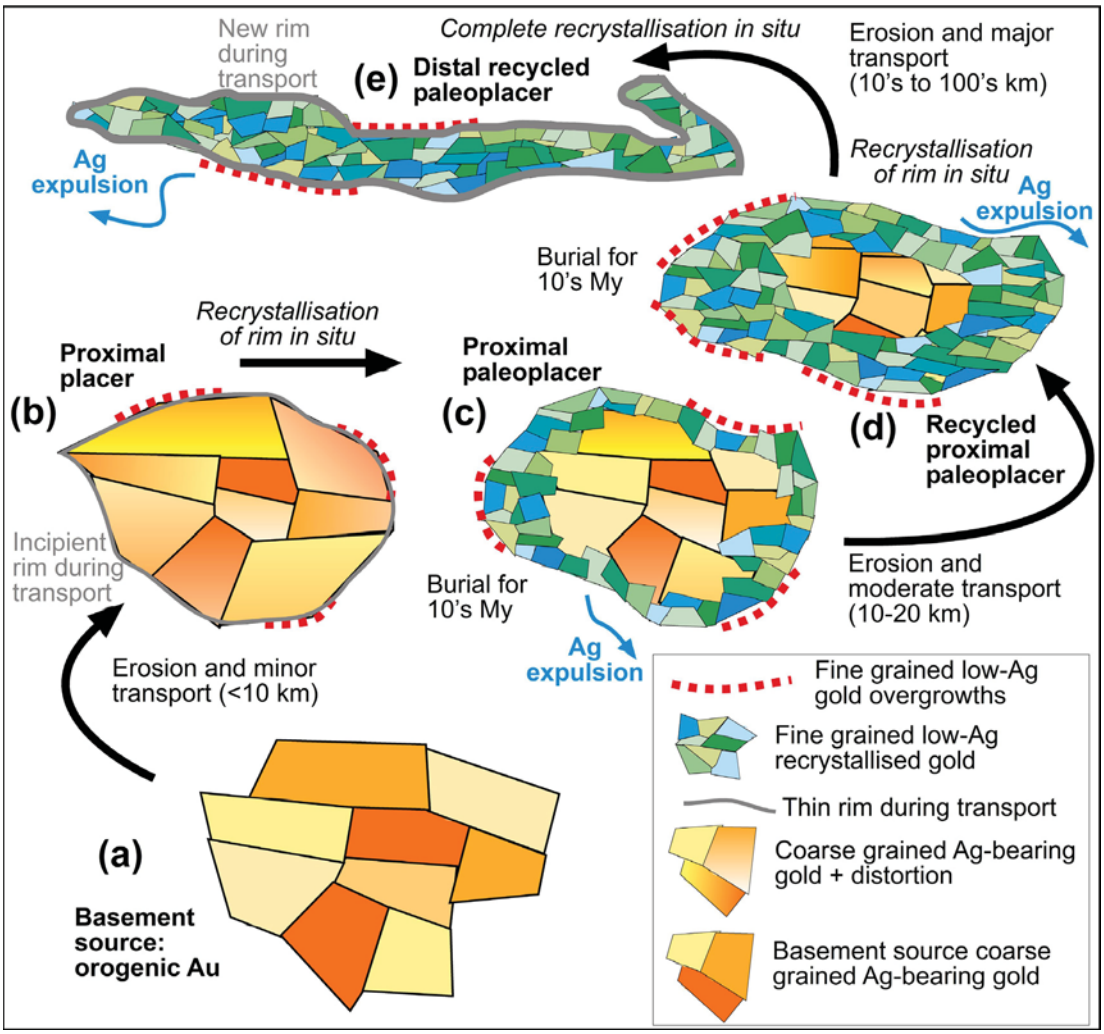

Fig. 10. Cartoon summary of inferred processes that result in progressive recrystallisation of detrital gold particles in paleoplacer deposits, based on observations of Eocene, Miocene and Cretaceous deposits of the Otago placer goldfield in this study. Deformation of gold grains (a–b) during transport results in strain-induced *in situ* recrystallisation after deposition (c–e), with associated expulsion in solution of some Ag. Minor additional rim formation also occurs in active rivers, followed by overgrowths after deposition, as in (e).

Acknowledgements

This research was supported by the Marsden Fund administered by the Royal Society of NZ; CSIRO Perth, Australia; Glass Earth Gold Ltd; NZ Ministry of Business Innovation and Employment; and the University of Otago. Kat Lilly at the Otago Centre for Electron Microscopy gave excellent assistance with the SEM, especially EBSD mapping. Discussions with Mark Hesson, Donna Falconer, Doug MacKenzie, and John Youngson were helpful in developing some of our ideas. Helpful and constructive reviews by Robert Scott and an anonymous referee substantially improved the presentation of the manuscript.

References

Beilby, G.T., 1903. Surface flow in crystalline solids under mechanical disturbance. Proc. Roy. Soc. London 72, 218–225.
Boyle, R.W., 1979. The geochemistry of gold and its deposits. Geol. Surv. Canada Bull. 280, 579.
Chapman, R.J., Mortensen, J.K., 2016. Characterization of gold mineralization in the Northern Cariboo Gold District, British Columbia, Canada, through integration of compositional studies of lode and detrital Gold with historical placer production: a template for evaluation of orogenic gold districts. Econ. Geol. 111, 1321–1345.
Chapman, R.J., Leake, R.C., Moles, N.R., Earls, G., Cooper, C., Harrington, K., Berzins, R., 2000. The application of microchemical analysis of gold grains to the understanding of complex local and regional gold mineralization: a case study in Ireland and Scotland. Econ. Geol. 95, 1753–1773.
Chapman, R.J., Mortensen, J.K., LeBarge, W.P., 2011. Styles of lode gold mineralization contributing to the placers of the Indian River and Black Hills Creek, Yukon Territory, Canada as deduced from microchemical characterization of placer gold grains. Mineral Deposita 46, 881–903.
Craw, D., 2010. Delayed accumulation of placers during exhumation of orogenic gold in southern New Zealand. Ore Geol. Rev. 37, 224–235.
Craw, D., 2013. River drainage reorientation during placer gold accumulation, southern New Zealand. Mineral Deposita 48, 841–860.
Craw, D., Lilly, K., 2016. Gold nugget morphology and geochemical environments of nugget formation, southern New Zealand. Ore Geol. Rev. 79, 301–315.
Craw, D., Smith, D.W., Youngson, J.H., 1995. Formation of authigenic Fe2+-bearing smectite-vermiculite during terrestrial diagenesis, southern New Zealand. NZ J. Geol. Geophys. 38, 151–158.
Craw, D., MacKenzie, D.J., Grieve, P., 2015. Supergene gold mobility in orogenic gold deposits, Otago Schist, New Zealand. NZ J. Geol. Geophys. 58, 123–136.
Craw, D., Hesson, M., Kerr, G., 2016. Morphological evolution of gold nuggets in proximal sedimentary environments, southern New Zealand. Ore Geol. Rev. 80, 784–799.
Desborough, G.A., 1970. Silver depletion indicated by microanalysis of gold from placer occurrences, western United States. Econ. Geol. 65, 304–311.
Doherty, R.D., Hughes, D.A., Humphreys, F.J., Jonas, J.J., Juul Jenson, D., Kassner, M.E., King, W.E., McNelley, T.R., McQueen, H.J., Rollett, A.D., 1997. Current issues in recrystallisation: a review. Mater. Sci. Eng. A238, 219–274.
Els, B.G., Youngson, J.H., Craw, D., 2003. Blue Spur Conglomerate: auriferous Late Cretaceous fluvial channel deposits adjacent to normal fault scarps, southeast Otago, New Zealand. NZ J. Geol. Geophys. 46, 123–139.

Fairbrother, L., Brugger, J., Shapter, J., Laird, J.S., Southam, G., Reith, F., 2012. Supergene gold transformation: biogenic secondary and nano-particulate gold from arid Australia. Chem. Geol. 320, 17–31.
Falconer, DM., Craw, D. 2009. Supergene gold mobility: a textural and geochemical study from gold placers in southern New Zealand. In: Titley, S.R. (Ed.), Supergene Environments, processes and products. Econ Geol Special Publ 14: 77–93.
Garnett, R.H.W., Bassett, N.C., 2005. Placer Deposits. Econ. Geol., 813–843 100th Anniv Vol..
Giusti, L., Smith, D.G.W., 1984. An electron microprobe study of some Alberta placer gold. Tschermaks Mineral. Petrogr. Mitt. 33, 187–202.
Groen, J.C., Craig, J.R., Rimstidt, R.D., 1990. Gold-rich rim formation on electrum grains in placers. Canad Mineral 28, 207–228.
Halfpenny, A., Hough, R.M., Verrall, M., 2013a. Preparation of samples with both hard and soft phases for electron backscatter diffraction: examples from gold mineralization. Microsc. Microanal. 19, 1007–1018.
Halfpenny, A., Hough, R.M., Nugus, M., 2013b. Crystallography of natural and synthetic gold alloy microstructures. Materal Sci. Forum 753, 477–480.
Henley, R.W., Adams, J., 1979. On the evolution of giant gold placers. Trans. Inst. Min. Metall. 88, B41–B50.
Hesson, M., Stewart, J., Stephens, S., Kerr, G., Craw, D., 2016. Gold nuggets in proximal placers, Old Man Range, Central Otago. Aus. Inst. Min. Metall. Monogr. 31, 359–366.
Jackson, J., Norris, R.J., Youngson, J.H., 1996. The structural evolution of active fault and fold systems in Central Otago, New Zealand: evidence revealed by drainage patterns. J. Struct. Geol. 18, 217–234.
Kerr, G., Malloch, K., Lilly, K., Craw, D., 2017. Diagenetic alteration of a Mesozoic fluvial gold placer deposit, southern New Zealand. Ore Geol. Rev. 83, 14–29.
Knight, J.B., Morison, S.R., Mortensen, J.K., 1999a. Lode and placer gold composition in the Klondike District, Yukon Territory, Canada: implications for the nature and genesis of Klondike placer and lode gold deposits. Econ. Geol. 94, 635–648.
Knight, J.B., Morison, S.R., Mortensen, J.K., 1999b. The relationship between placer gold particle shape, rimming, and distance of fluvial transport as exemplified by gold from the Klondike district, Yukon Territory, Canada. Econ. Geol. 94, 635–648.
Landis, C.A., Campbell, H.J., Begg, J.G., Mildenhall, D.C., Paterson, A.M., Trewick, S.A., 2008. The Waipounamu erosion surface: questioning the antiquity of the New Zealand land surface and terrestrial fauna and flora. Geol. Mag. 145, 173–197.
Little, T.A., Prior, D.J., Toy, V.G., 2015. Are quartz LPOs predictably oriented with respect to the shear zone boundary?: A test from the Alpine Fault mylonites, New Zealand. Geochem. Geophys. Geosyst. 17, 981–999.
Mayerhofer, T.G., 2005. Symmetric Euler orientation representations for orientational averaging. Spectrochim. Acta A61, 2611–2621.
McClenaghan, M.B., Cabri, L.J., 2011. Review of gold and platinum group element (PGE) indicator minerals methods for surficial sediment sampling. Geochem.: Exp. Environ. Anal. 11, 251–263.
Nolze, G., 2015. Euler angles and crystal symmetry. Cryst. Res. Technol. 50, 188–201.
Prior, D.J., Boyle, A.P., Brenker, F., Cheadle, M.C., Day, A., Lopez, G., Peruzzo, L., Potts, G.J., Reddy, S., Spiess, R., 1999. The application of electron backscatter diffraction and orientation contrast imaging in the SEM to textural problems in rocks. Am. Mineral. 84, 1741–1759.
Prior, D.J., Mariani, E., Wheeler, J., 2009. EBSD in the Earth Sciences: applications, common practice and challenges. In: Schwartz, A.J., Kumar, M., Adams B.L., Field, D.P., (Eds.), Electron Backscatter Diffraction in Materials Science. second ed., Springer. Chapter 29, pp. 345–357.
Reith, F., Lengke, M.F., Falconer, D., Craw, D., Southam, G., 2007. Winogradsky review: the geomicrobiology of gold. ISME J. 1, 567–584.
Reith, F., Stewart, L., Wakelin, S.A., 2012. Supergene gold transformation: secondary and nano-particulate gold from southern New Zealand. Chem. Geol. 320, 32–46.
Shuster, J., Reith, F., Cornelis, G., Parsons, J.E., Parson, J.M., Southam, G., 2017. Secondary gold structures: relics of past biogeochemical transformations and implications for colloidal gold dispersion in subtropical environments. Chem. Geol. 450, 154–164.
Townley, B.K., Herail, G., Maksaev, V., Palacios, C., de Parseval, P., Sepuldeva, F., Orellana, R., Rivas, P., Ulloa, C., 2003. Gold grain morphology and composition as an exploration tool application to gold exploration in covered areas. Geochem.: Exp. Environ. Anal. 3, 29–38.
Turnbull, I.M. 2000. Geology of the Wakatipu area. Institute of Geological & Nuclear Sciences 1:250 000 geological map 18. 1 sheet + 72p. Lower Hutt, New Zealand. Inst Geol Nuclear Sci.
Webster, J.G., 1986. The solubility of Au and Ag in the system Au–Ag–S–O_2–H_2O at 25 °C and 1 atm. Geochim. Cosmochim. Acta 50, 245–255.
Williams, G.J., 1974. Economic Geology of New Zealand. Austral Inst Min Metall Monograph 4, 490 p.
Youngson, J.H., Craw, D., 1993. Gold nugget growth during tectonically induced sedimentary recycling, Otago, New Zealand. Sed. Geol. 84, 71–88.
Youngson, J.H., Craw, D., 1999. Variation in placer style, gold morphology, and gold particle behaviour down gravel bed-load rivers: an example from the Shotover/Arrow-Kawarau-Clutha River system, Otago, New Zealand. Econ. Geol. 94, 615–634.
Youngson, J.H., Craw, D., Falconer, D.M., 2006. Evolution of Cretaceous-Cenozoic quartz pebble conglomerate gold placers during basin formation and inversion, southern New Zealand. Ore Geol. Rev. 28, 451–474.